

Spatial variability of thermal properties in relation to the application of selected soil-improving cropping systems (SICS) on sandy soil**

Bogusław Usowicz^{1,2*}  and Jerzy Lipiec¹ 

¹Institute of Agrophysics, Polish Academy of Sciences, Doświadczalna 4, 20-290 Lublin, Poland

²Faculty of Civil Engineering and Environmental Sciences, Białystok University of Technology, Wiejska 45 E, 15-351 Białystok, Poland

Received June 14, 2022; accepted July 14, 2022

Abstract. The study aimed to determine the effect of randomly applied soil-improving cropping systems on the variability of soil thermal conductivity, heat capacity, and thermal diffusivity over the course of a 3-year (2016-2018) study. The field experiment included the control and the following soil-improving cropping systems: liming, leguminous catch crops for green manure, farmyard manure, and liming+leguminous catch crops+farmyard manure together with spring oats (2017) and spring wheat (2018). The parameters such as bulk density, water content, and values of soil thermal conductivity, heat capacity, and thermal diffusivity have been determined. The thermal properties were measured at the current water content in situ and in water-saturated and dry soil states in the laboratory. The thermal properties in the wet year of 2017 increased in the subareas with a predominance of leguminous catch crops for green manure, farmyard manure, and liming+leguminous catch crops+farmyard manure, whereas the soil-improving cropping systems effect was not consistent after stubble tilling in the dry year of 2018. Cross-semivariograms which used the sand content as an auxiliary variable and cokriging produced a better prediction than the semivariograms and kriging. The fractal analysis indicated that the number of subareas differing in thermal properties was mainly modified by water content

and bulk density. The spatial spread of the soil thermal properties during the water-saturated and dry states increased in subareas with a higher bulk density.

Keywords: soil-improving practices, thermal conductivity, heat capacity, thermal diffusivity, semi- and cross-semivariograms, kriging and cokriging, mapping

INTRODUCTION

Soil thermal properties, including thermal conductivity, thermal diffusivity, and heat capacity are the primary factors governing surface-energy partitioning and heat transfer in the soil profile (Ochsner *et al.*, 2007; Lipiec and Hatano, 2003; Liu *et al.*, 2018). In addition, they influence soil water conditions through the effect of latent heat exchange and evaporation (Heitman *et al.*, 2020). Heat transfer and the temperature distribution of the soil have important effects on seedling growth and its associated crop establishment (Abu-Hamdeh and Reeder, 2000; Mellander *et al.*, 2004; Lipiec *et al.*, 2011), microbial respiration rate, organic matter turnover (Andry *et al.*, 2009; Xu *et al.*, 2012), and greenhouse gas exchange (Peng *et al.*, 2009; Xu *et al.*, 2012). The measured soil thermal properties are required in coupled heat and water transfer models (Heitman *et al.*, 2008; Tarnawski *et al.*, 2021) in order to improve the prediction of the spatial and temporal dynamics of soil temperature and the effects

*Corresponding authors e-mail: b.usowicz@ipan.lublin.pl

**This work was partially funded by HORIZON 2020, the European Commission, Programme: H2020-SFS-2015-2: SoilCare for profitable and sustainable crop production in Europe, project No. 677407 (SoilCare, 2016-2021) and by WZ/WB-INL/3/2021 from the science funds from the Ministry of Science and Higher Education in Poland.

of land management practices under climate change conditions (Zhao and Sia, 2019). The exploration of the spatial variability in soil thermal properties is important in predicting ecosystem function and precision agriculture (Usowicz *et al.*, 2017; Mitchell-Fostyk *et al.*, 2021). A knowledge of soil thermal properties is also useful in studying space conditions where soils are used as an analogue of extra-terrestrial porous media (Usowicz *et al.*, 2008; Nagihara *et al.*, 2014).

The thermal properties of different soil types are for the most part determined by the composition of the solid phase, including the content of mineral particles and soil organic matter (Gamage *et al.*, 2019; Schjønning, 2021; Mitchell-Fostyk *et al.*, 2021). However, these properties of a given soil type are largely dependent on the variable parameters of soil water status, air-filled porosity (Ochsner *et al.*, 2001; Lipiec and Hatano, 2003) and bulk density (Dec *et al.*, 2009; Usowicz *et al.*, 2013), and on the less variable organic matter content (Abu-Hamdeh and Reeder, 2000). Even small alterations in soil composition may have a substantial effect on soil heat conduction, as the thermal conductivity and diffusivity of air as compared to other soil components are many-fold lower (Liu *et al.*, 2018). Therefore, soil thermal conductivity was more closely correlated with air-filled porosity than with the volume fraction of water (Usowicz, 1995; Ochsner *et al.* (2001). A recent study conducted by Schjønning (2021) on different soils has revealed that thermal conductivity during dry and water-saturated states had a wider range than those reported in the literature. In dry conditions thermal conductivity is a critical parameter in the model predicting conductivity based on the normalized concept (He *et al.*, 2021; Schjønning, 2021). Therefore, further measurements of the conductivity in soils with an undisturbed structural composition over a range of soil water conditions are required.

Soil compaction, composition, and the number of contacts between soil particles can be altered by the application of soil-improving cropping systems (SICS), *e.g.* organic amendments, extended crop rotation with cover crops (Ajayi *et al.*, 2016; Bolinder *et al.*, 2020), or liming favouring the formation of a more diversified and stable soil structure and pore-size distribution (Krasowicz *et al.*, 2011; Keiblinger *et al.*, 2016). Increasing the soil organic matter content and greening associated with the use of catch crops forms a part of the global strategy to improve carbon sequestration stocks (Yost and Hartemink, 2019; Bolinder *et al.*, 2020; Valkama *et al.*, 2015; Zaniewicz-Bajkowska *et al.*, 2013) and mitigate global warming effects (Soussana *et al.*, 2017; Lal, 2020). However, at present there is a lack of data available concerning the effects of SICS on the thermal properties of soil. Some studies have shown that the application of biochar and recycled organic materials increases the thermal conductivity and thermal diffusivity also increases with increasing soil water content (Liu *et al.*, 2018; Usowicz *et al.*, 2016; Usowicz and Lipiec, 2019); this effect was more pronounced in soil with a greater rather

than a lower bulk density (Usowicz *et al.*, 2016). However, at controlled and similar soil water contents, the thermal capacity and conductivity decreased in response to biochar addition mainly due to the increase in soil porosity (Liu *et al.*, 2018; Usowicz *et al.*, 2020).

The application of SICS is of particular importance on sandy soils with low quality and productivity that are for the most part characterized by a low organic matter content, water-holding capacity, and acidity. At the same time, the soils are characterized by a low heat capacity which is associated with large daily temperature fluctuations (Akter *et al.*, 2015), these increase the risk of plant injury caused by extreme temperatures (Lipiec *et al.*, 2011). Instead, they warm up rapidly in the spring prior to the growing season to achieve the minimum soil temperature required for plant growth (Akter *et al.*, 2015; Gliński and Lipiec, 1990) and require rather low energy inputs for tillage (Novák *et al.*, 2014). On a global basis, sandy soils occupy around 900 million ha⁻¹ (Yost and Hartemink, 2019) and occur in different regions across the world (Bronick and Lal, 2005; Thorsen *et al.*, 2010; Jankowski *et al.*, 2011). In Poland, around half of all soils were formed from sands of a glacial origin (Białousz *et al.*, 2005; Rutkowska and Pikuła 2013). In spite of their low quality, sandy soils are progressively being used for crop production due to a deficiency in agricultural land resources (Yost and Hartemink, 2019; Schjønning *et al.*, 2009; Usowicz and Lipiec, 2017) and the rising global population and food demand (Reichert *et al.*, 2009; Lal, 2020).

These data indicate that SICS may have a substantial effect on soil thermal properties. To the best of our knowledge, no comprehensive studies have been performed as yet to assess the spatial distribution of soil thermal properties upon SICS application on sandy soils. Therefore, the aim of this study was to determine the effect of various randomly applied soil-improving practices such as liming, catch crops, and farmyard manure on the spatial variability of soil thermal conductivity, heat capacity, and thermal diffusivity with particular consideration of the distribution of soil physical properties over a 3-year trial in field and laboratory conditions.

MATERIALS AND METHODS

The field study (350×40 m) was located on a private farm in Szaniawy, which is in the Podlasie region, Poland (51°59'09.8"N, 22°33'57.5"E) on Podzol soil (WRB, 2015) it is derived from a sandy material of glacial origin. Most of the soils in the study area are used in crop production. A tillage system with mouldboard ploughing (20-25 cm) dominates in the study area. Crop rotation includes cereals for the most part and, to a lesser degree, potatoes and legumes. Small wheeled tractors (up to 3.5 Mg) and combine harvesters (up to 10 Mg) are commonly used in the study area and do not cause heavy soil compaction. These management practices have been used over the course of the

last three decades (Usowicz *et al.*, 2004). The randomized experiment (Fig. 1) was started in the autumn of 2016 with oats (*Avena sativa* L.) in 2017 and wheat (*Triticum aestivum* L.) in 2018. These crops predominate in the crop rotation of the study area. The treatments were as follows: (C) control, (L) liming with 5.6 t ha⁻¹ CaCO₃ (applied once in the autumn of 2016), (LU) catch crops for green manure including yellow lupine (*Lupinus luteus* L.), serradella (*Ornithopus sativus*) and phacelia (*Phacelia tanacetifolia* Benth) that are grown every year (with respective seeding rates of 130, 30, and 3 kg ha⁻¹), (M) farmyard manure at 30 t ha⁻¹ every year in the autumn, and (L+LU+M) liming (as in treatment L) + catch crops (as in treatment LU) + manure (10 t ha⁻¹). Yellow lupine, serradella, and phacelia are often used as green manures in Poland. Each treatment consisted of three plots (20×40 m) separated by a 1.0 m margin.

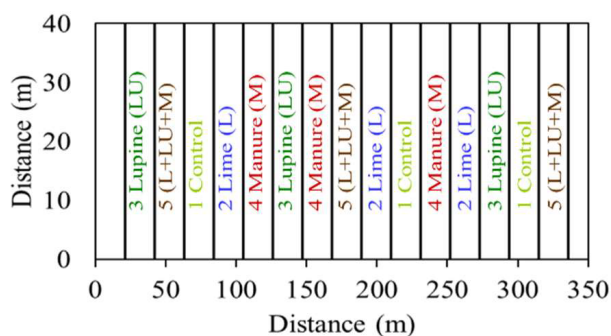


Fig. 1. Arrangement of the field plot with the following soil-improving cropping systems (SICS) applied: 1 – control, 2 – lime (L), 3 – leguminous catch crops (LU), 4 – farmyard manure (M), and 5 – lime + leguminous catch crops + farmyard manure (L+LU+M).

The measurements comprised the particle size distribution with Bouyoucos's sedimentation technique which was modified by Casagrande and Prószyński (ISO, 1995), organic carbon using the Tiurin titration technique (Ostrowska *et al.*, 1991), cation exchange capacity through the neutralization of the acidic groups with barium chloride (ISO, 1995), and pH in 1M KCl using the combination pH electrode of Orion Research. These parameters were determined in 150 soil samples (layer 0-25 cm) evenly covering the whole field area (350×40 m) at the beginning of experiment in 2016.

The measurements or calculations during the experiment were carried out on three different occasions, including a few days after cereal harvest in 2016 (25 August) and 2017 (24 August) and after stubble tilling and sowing catch crops in 2018 (16 October). They included dry bulk density (BD) using soil cores of 100 cm³ and 5 cm in diameter (Blake and Hartge, 1986), the particle density (Mg m⁻³) was calculated from the following relationship: bulk density/(1 – total porosity) where the total porosity was equal to the saturated water content at pF 0 (*i.e.*, log₁₀ (|1 cm H₂O|)). The gravimetric volumetric water content (WC) was determined using the same soil cores as for the determination of the dry bulk density. Measurements of the volumetric water content in the field were performed using a TDR meter (WCT). The

gravimetric vs. TDR soil water contents were higher and exhibited a lower error (WC vs. WCT < ~ 2%); therefore, they were used in further analyses. All of the soil measurements were made at 45 points (WC) and 90 points (WCT) in a grid covering the whole field area in an approximately even manner.

Measurements of the thermal conductivity (K), heat capacity (Cv), and thermal diffusivity (D) of the soils were performed at the current soil water content in the field using a KD2 Pro meter (Decagon Devices). Additionally, laboratory measurements of K, Cv, and D were made at the current soil water content at both dry and water-saturated states using the same KD2 Pro meter and 100 cm³ soil cores. Both field and laboratory measurements were carried out at 90 points (5 treatments × 18 replicates taken randomly). Measurements of all soil properties were conducted at a depth of 0-10 cm.

The spatial dependence and distribution for soil thermal (z_1) and physical properties (z_2) were determined using geostatistical methods (Gamma Design Software, GS+9, Robertson, 2008). The experimental semivariogram $\gamma(h)$ and cross-semivariogram between the soil thermal (z_1) and physical properties (z_2) – $\gamma_{12}(h)$ for the distance h (m) were obtained from the following equations:

$$\gamma(h) = \frac{1}{2N(h)} \sum_{i=1}^{N(h)} [z_1(x_i) - z_1(x_i + h)]^2, \quad (1)$$

$$\gamma_{12}(h) = \frac{1}{2N(h)} \sum_{(i=1)}^{N(h)} [z_1(x_i) - z_1(x_i + h)][z_2(x_i) - z_2(x_i + h)], \quad (2)$$

where: $N(h)$ is the number of pairs of points with values of $[z_1(x_i), z_1(x_i + h)]$, $[z_2(x_i), z_2(x_i + h)]$, separated by a distance h , and x_i is the location coordinate. For the semivariograms and cross-semivariograms obtained empirically, the exponential model was fitted (Robertson, 2008):

$$\gamma_{12}(h) = C_0 + C \left[1 - e^{-\frac{|h|}{A_0}} \right] |h| > 0, \quad (3)$$

where: $\gamma(h)$ is the semivariance for the inner distance class h , h is the lag distance interval, C_0 is the nugget variance ≥ 0 , C is the structural variance $\geq C_0$, A_0 is the range parameter, and $C_0 + C$ is the sill. As for the exponential isotropic model, the effective range $A = 3A_0$, that is the distance where the sill ($C + C_0$) is inside 5% of the asymptote.

The gained mathematical functions of the semivariograms and cross-semivariograms were used for spatial analysis and also for graphical visualization through the estimation of the thermal and physical properties of the soil using kriging or cokriging methods. Experimental semivariograms and cross-semivariograms were obtained from the measured data of soil thermal and physical properties. Then, parameters and models with the minimum residual sum of squares and the highest R² values were fitted to the experimental semivariograms and cross-semivariograms.

Ordinary cokriging (OCK) and ordinary kriging (OK) were used to predict the spatial distribution of soil thermal properties and selected soil physical properties,

respectively. The estimator of kriging and cokriging are linear equations which may be expressed by the following formula (Robertson, 2008):

$$z^*(x_o) = \sum_{i=1}^N \lambda_i z(x_i), \quad (4)$$

$$z_2^*(x_o) = \sum_{i=1}^{N_1} \lambda_{1i} z_1(x_{1i}) + \sum_{j=1}^{N_2} \lambda_{2j} z_2(x_{2j}), \quad (5)$$

where: N is the number of measurements, $z(x_i)$ – the value measured at point x_i , $z^*(x_o)$ – the estimated value at the point of estimation x_o , and λ_i – the weights, and λ_{1i} and λ_{2j} are the weights associated with z_1 and z_2 . N_1 and N_2 are the numbers of neighbours of z_1 and z_2 used for the estimation at point x_o .

In our study, the ordinary cokriging technique was used to enhance the estimation of the spatial distribution of soil thermal properties using sparse sampling data of the soil thermal properties and denser sampling data of the sand content as an auxiliary variable. Cross-validation analysis was applied for evaluating the extent of the agreement between the measured values and those estimated using kriging and cokriging methods.

Figure 2 illustrates the course of the monthly mean air temperatures and rainfall sums for the years 2016, 2017, and 2018 at the study site. The average growing season

temperatures (April-September) and the annual temperatures in successive years were 15.5, 14.8, 17.1°C and 8.7, 8.7, 9.3°C, respectively. In 2017 the growing season temperatures proved to be among the lowest during the past 50-year period with a maximum of 16.3°C. The growing season and annual precipitation in 2016, 2017, and 2018 were 341.7, 424.1, 308.1 mm and 718.0, 670.1, 509.1 mm, respectively. During the three growing seasons the precipitation values were below the long-term average (567 mm).

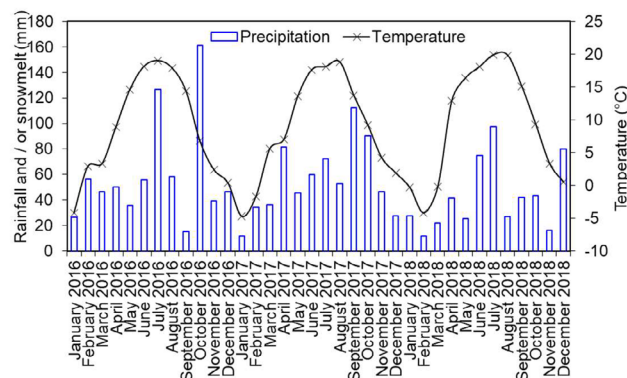


Fig. 2. Monthly precipitation sums and average air temperatures in the study years. Arrow bars indicate the months of the growing seasons.

Table 1. Basic statistics of soil texture, organic carbon content (OC), cation-exchange capacity (CEC) (0-25 cm), bulk density (BD), porosity (FI), particle density (PD), TDR water content (WCT), and gravimetric water content (WC) in the 0-10 cm layer in the field

	Sand (%)	Silt (%)	Clay (%)	OC (%)	CEC (cmol kg ⁻¹)	BD (Mg m ⁻³)	FI (m ³ m ⁻³)	PD (Mg m ⁻³)	WCT (m ³ m ⁻³)	WC (m ³ m ⁻³)
Date	25.08.2016									
Number	150	150	150	150	150	45	45	45	90	45
Mean	62.9	34.8	2.2	0.80	12.3	1.537	0.373	2.45	0.205	0.214
SD	5.1	4.8	1.15	0.23	2.8	0.078	0.028	0.04	0.022	0.019
CV (%)	8.1	13.9	51.8	28.9	22.6	5.1	7.6	1.6	10.8	9.0
Minimum	53.0	18.0	0.0	0.13	4.8	1.381	0.323	2.38	0.13	0.162
Maximum	81.0	45.0	6.0	1.52	21.3	1.675	0.429	2.55	0.255	0.255
Skewness	0.974	-0.930	0.849	0.144	0.514	-0.379	0.328	0.351	-0.885	-0.546
Kurtosis	0.793	0.920	1.054	0.892	0.700	-0.861	-0.884	-0.836	1.195	0.245
	BD (Mg m ⁻³)	FI (m ³ m ⁻³)	PD (Mg m ⁻³)	WCT (m ³ m ⁻³)	WC (m ³ m ⁻³)	BD (Mg m ⁻³)	FI (m ³ m ⁻³)	PD (Mg m ⁻³)	WCT (m ³ m ⁻³)	WC (m ³ m ⁻³)
Date	24.08.2017					16.10.2018				
Number	45	45	45	90	45	45	45	45	90	45
Mean	1.551	0.385	2.523	0.190	0.230	1.286	0.447	2.328	0.058	0.091
SD	0.108	0.029	0.132	0.022	0.022	0.079	0.021	0.104	0.014	0.013
CV (%)	7.0	7.6	5.2	11.8	9.7	6.2	4.7	4.5	24.1	14.7
Minimum	1.289	0.338	2.284	0.134	0.180	1.075	0.368	2.024	0.027	0.050
Maximum	1.728	0.448	2.704	0.226	0.267	1.509	0.486	2.491	0.085	0.118
Skewness	-0.601	0.762	-0.167	-0.531	-0.403	-0.018	-1.036	-1.055	-0.301	-0.480
Kurtosis	-0.275	-0.462	-1.502	-0.217	-0.598	0.690	2.376	0.867	-0.529	0.399

Sand (2-0.05 mm), silt (0.05-0.002 mm) and clay (<0.002 mm), SD – standard deviation, CV (%) – coefficient of variation.

RESULTS

The mean contents of sand, silt, clay, organic carbon (OC) and the values of the cation-exchange capacity (CEC) and particle density in the top 0-25 cm of the soil were 62.9, 34.8, 2.2, 0.80%, 12.3 cmol kg⁻¹, and 2.45 Mg m⁻³, respectively (Table 1) (Usovicz and Lipiec, 2022). The corresponding coefficients of variation (CV) were 8.1, 13.9, 51.8, 28.0, 22.6, and 1.6%. The means and CVs of bulk density (BD), total porosity (FI), TDR water content (WCT), and gravimetric water content (WC) differed depending on the study year (Table 1). The means of BD and FI measured at harvest time were similar in 2016-2017 with respective ranges of 1.537-1.551 Mg m⁻³ and 0.373-0.385 m³ m⁻³ and a low CV from 5.1 to 7.6% for both. In 2018, the mean BD measured after stubble tilling decreased to 1.286 Mg m⁻³ and FI increased to 0.447 m³ m⁻³, whereas the CVs remained similarly low (4.7-6.2%). The means of WCT determined with TDR and gravimetric WC varied

from 0.190 to 0.230 m³ m⁻³ in 2016-2017 and from 0.058 to 0.091 m³ m⁻³ in 2018. The corresponding ranges of CVs were 5.2-1.8% and 14.7-24.1%. In most cases, the CVs were classified as low (0-15%), except for the medium value (15-75%) for the content of clay, OC, WCT, and CEC in 2018 (Dahiya *et al.*, 1984).

The positive skewness of the values indicates that the distribution of sand, clay, OC contents, CEC, and PD in 2016 and porosity in 2016-2017 had a positive asymmetry, whereas the silt content in 2016 and particle density in 2017 had a negative asymmetry. The asymmetry of BD, WC, and WCT was negative in both 2016 and 2017. In 2018, the skewness of all of the soil properties was negative. The distribution for all three textural fractions, WC, and WCT in 2016 as well as BD and PD in 2018 was slender (kurtosis values > 0 (0.245-2.376)) and flattened for BD, FI, and PD in 2016-2017 and for WC and WCT in 2017 (-1.502 to -0.217). The square root transformation and the natural logarithm of

Table 2. Basic statistics of thermal conductivity – K (W m⁻¹ K⁻¹), heat capacity – Cv (MJ m⁻³ K⁻¹), thermal diffusivity – D (mm² s⁻¹) in the 0-10 cm layer at the current soil water content in the field (columns 2-4) and at dry and water-saturated (sat.) states

	K (W m ⁻¹ K ⁻¹)	Cv (MJ m ⁻³ K ⁻¹)	D (mm ² s ⁻¹)	K _{dry} (W m ⁻¹ K ⁻¹)	Cv _{dry} (MJ m ⁻³ K ⁻¹)	D _{dry} (mm ² s ⁻¹)	K _{sat.} (W m ⁻¹ K ⁻¹)	Cv _{sat.} (MJ m ⁻³ K ⁻¹)	D _{sat.} (mm ² s ⁻¹)
Number	90	90	90	45	45	45	45	45	45
Date	25.08.2016								
Mean	1.640	2.936	0.570	0.324	1.721	0.195	1.900	3.537	0.540
SD	0.245	0.503	0.109	0.044	0.321	0.047	0.159	0.298	0.058
CV (%)	14.9	17.1	19.1	13.7	18.6	24.3	8.4	8.4	10.7
Minimum	1.047	1.373	0.396	0.238	1.152	0.113	1.532	2.570	0.435
Maximum	2.124	3.952	1.021	0.414	2.931	0.356	2.160	4.062	0.809
Skewness	-0.199	-0.074	1.254	-0.014	1.134	0.780	-0.450	-0.610	1.825
Kurtosis	-0.686	-0.411	2.135	-0.674	2.890	1.292	-0.732	0.800	7.699
Date	24.08.2017								
Mean	1.391	2.897	0.482	0.311	2.058	0.155	1.804	3.797	0.469
SD	0.284	0.549	0.062	0.044	0.337	0.031	0.159	0.319	0.064
CV (%)	20.4	19.0	12.8	14.2	16.4	19.9	8.8	8.4	13.7
Minimum	0.698	1.452	0.367	0.224	1.490	0.093	1.217	2.707	0.371
Maximum	1.996	4.013	0.730	0.406	3.163	0.272	2.115	4.010	0.741
Skewness	-0.125	0.087	1.012	0.242	1.110	0.684	-0.829	-0.623	1.595
Kurtosis	-0.841	-0.391	1.394	-0.246	1.740	2.868	2.307	0.292	4.510
Date	16.10.2018								
Mean	0.548	1.382	0.390	0.213	1.202	0.183	1.489	2.681	0.562
SD	0.223	0.220	0.129	0.030	0.202	0.045	0.130	0.257	0.090
CV (%)	40.6	15.9	33.0	14.2	16.8	24.4	8.7	9.6	15.9
Minimum	0.171	0.899	0.154	0.149	0.861	0.134	1.194	1.993	0.432
Maximum	1.336	2.360	0.829	0.296	1.807	0.331	1.893	3.192	0.950
Skewness	0.988	0.682	1.069	0.730	0.728	1.517	0.580	-0.457	1.913
Kurtosis	1.078	1.697	1.544	0.452	0.650	2.175	0.906	0.167	5.616

K – thermal conductivity, Cv – heat capacity, D – thermal diffusivity from field measurements.

the data with properties that exhibited asymmetry did not improve the extent of the agreement with the normal distribution; therefore, it was assumed that the untransformed data distributions were close to the normal distribution and could therefore be used in the geostatistical analysis.

The mean soil thermal conductivity (K) measured *in situ* had the highest value in 2016 ($1.64 \text{ W m}^{-1} \text{ K}^{-1}$) and decreased in 2017 and 2018 to 1.39 and $0.548 \text{ W m}^{-1} \text{ K}^{-1}$, respectively (Table 2). The thermal diffusivity (D) also decreased in the following years from 0.57 to $0.39 \text{ mm}^2 \text{ s}^{-1}$. The heat capacity (Cv) remained almost the same ($\approx 2.9 \text{ MJ m}^{-3} \text{ K}^{-1}$) in 2016-2017 and appreciably decreased to $1.38 \text{ MJ m}^{-3} \text{ K}^{-1}$ in 2018. The range of thermal conductivity and thermal diffusivity of the CVs was 12.8-20.4% in 2016-2017, whereas in 2018 it was 33.0-40.6%. The range of the soil heat capacity CVs was 17.1-19% for all of the years of the study.

The thermal conductivity of the dry and water-saturated soil decreased in the following study years (2016-2018) from $0.32 \text{ W m}^{-1} \text{ K}^{-1}$ to 0.213 and from 1.9 to $1.489 \text{ W m}^{-1} \text{ K}^{-1}$, respectively. The thermal diffusivities of the dry and water-saturated soil were lower in 2017 (0.155 and $0.469 \text{ mm}^2 \text{ s}^{-1}$, respectively) compared to those of 2016 (0.195 and $0.540 \text{ mm}^2 \text{ s}^{-1}$) and 2018 (0.184 and $0.562 \text{ mm}^2 \text{ s}^{-1}$). The heat capacity, in contrast to the thermal diffusivity, was higher in 2017 for both dry and water-saturated states (2.058 and $3.797 \text{ MJ m}^{-3} \text{ K}^{-1}$, respectively) as compared to those in 2016 (1.72 and $3.54 \text{ MJ m}^{-3} \text{ K}^{-1}$) and 2018 (1.202 and $2.681 \text{ MJ m}^{-3} \text{ K}^{-1}$). The thermal conductivity, heat capacity, and thermal diffusivity CVs of the dry soil were 13.7-14.2, 16.4-18.6, and 19.9-24.4%, respectively, regardless of the year of the study. The corresponding ranges in the water-saturated soil were 8.4-8.8, 8.4-9.6, and 10.7-15.9%.

The distributions of the thermal conductivity and heat capacity measured *in situ* were slightly left-hand side oblique (in 3 out of 4 cases) (from -0.199 to 0.087) and slightly flattened (kurtosis from -0.841 to -0.391) in 2016-2017. The distributions of the thermal diffusivity measured *in situ* in 2016 and 2017 and all of the thermal properties measured after stubble tilling in 2018 exhibited right-hand side asymmetry. In the dry state, the distributions of the thermal properties in 2016-2017 were generally right-handed (from -0.014 to 1.134), whereas the distribution in the water-saturated soil was left-handed for thermal conductivity and heat capacity (from -0.829 to -0.610) and right-handed for thermal diffusivity (1.825 and 1.595). In 2018, all of the thermal properties in the dry and saturated states were right-handed, except for the left-handed distribution of the heat capacity. In most cases, the distributions in both states were slender (kurtosis >0).

The experimental values of the semi- and cross-semivariograms for all soil properties were best fitted to exponential models (in most cases ($0.3 < R^2 < 0.9$)). The nugget (C_0) values in semivariograms were relatively low for pH (KCl), OC, BD, FI, PD, WC, WCT, K, Cv, and D and varied from 0.0 to 0.0504 (Figs 3-6), except for the range from 0.1 to around 10

for sand, silt, clay, and CEC, where they were considerably higher (Usowicz and Lipiec, 2022). The sill values (C_0+C) also ranged from 0.002 to 0.317 except for sand, silt, clay, and CEC (from 1.5 to 32). The effective ranges (A) of the spatial dependence in semivariograms were the greatest for sand and silt (about 130 m) and decreased for clay and CEC <40 m and also for pH, OC <20 m (Usowicz and Lipiec, 2022). The effective ranges (A) of the spatial dependence were from 34 to 103 m for BD, from 32 to 80 m for FI, from 31 to 120 m for PD, and from 21 to 114 m for WC and WCT. The effective ranges of the field-measured thermal properties varied from 10.5 to 27.6 m and those of the laboratory measurements in the dry and water-saturated states ranged from 12.9 to 115 m (Figs 3-6). The values of relative structural variance ($C_0/(C_0 + C)$) of below 0.25 for all soil and thermal properties indicate a very close spatial dependence and those in the range of 0.25-0.75 for sand and silt imply moderate spatial dependence (Cambardella *et al.*, 1994).

As for the cross-semivariograms, the nugget (C_0) values for the thermal soil properties measured in the field and laboratory (for both dry and water-saturated soils) (paired K, Cv, D with sand, silt, clay, pH (KCl), OC, CEC, BD, FI, PD, WC, and WCT) were positive (from 0.0001 to 0.0227) in 155 cases and negative (from -0.0231 to -0.0001) in the remaining 133 cases (Figs 3-6). In general, negative nugget values were found for the thermal properties paired with total porosity (23 out of 27 cases), sand (13 out of 27 cases), silt (15 out of 27), clay (16 out of 27), and less frequently for the remaining cases. The corresponding sill values ranged from 0.105 to 0.525 and from -0.383 to -0.0746 , respectively. The ranges of spatial dependence varied from 7.5 to 140 m for thermal properties paired with soil properties and from 10.5 to 115 m for soil thermal properties alone (Figs 3-6). The spatial dependence (ratios of $C_0/(C_0+C)$) (nugget/sill) for all thermal properties alone and for thermal properties paired with soil properties for field and laboratory measurements were < 0.25 in most cases (284) and 0.260-0.429 in the remaining 4 cases, thereby indicating close and moderate spatial dependence, respectively (Cambardella *et al.*, 1994). It is worth noting that the spatial dependences (nugget/sill) were closer for most of the cross-semivariograms as compared to the semivariograms.

The fractal dimensions (D0) of the soil and the thermal properties in the experimental field with different SICS were determined with good agreement between them (coefficients of determinations > 0.8). As may be observed in Fig. 6, the fractal dimensions ranged from approximately 1.534 to over 1.982 for stable soil properties, including sand, silt, clay, pH, OC, and CEC and from 1.760 to 1.942 for the relatively stable (BD, FI) and variable (WC, WCT) properties. Particle density (PD) had the lowest (1.534) value indicating a smoother (less diverse) distribution (Fig. 6). The fractal dimensions for all of the thermal properties ranged from 1.962 to 1.997 in the field, from 1.679 to 1.955 in the dry soil, and from 1.814 to 1.980 in water-saturated

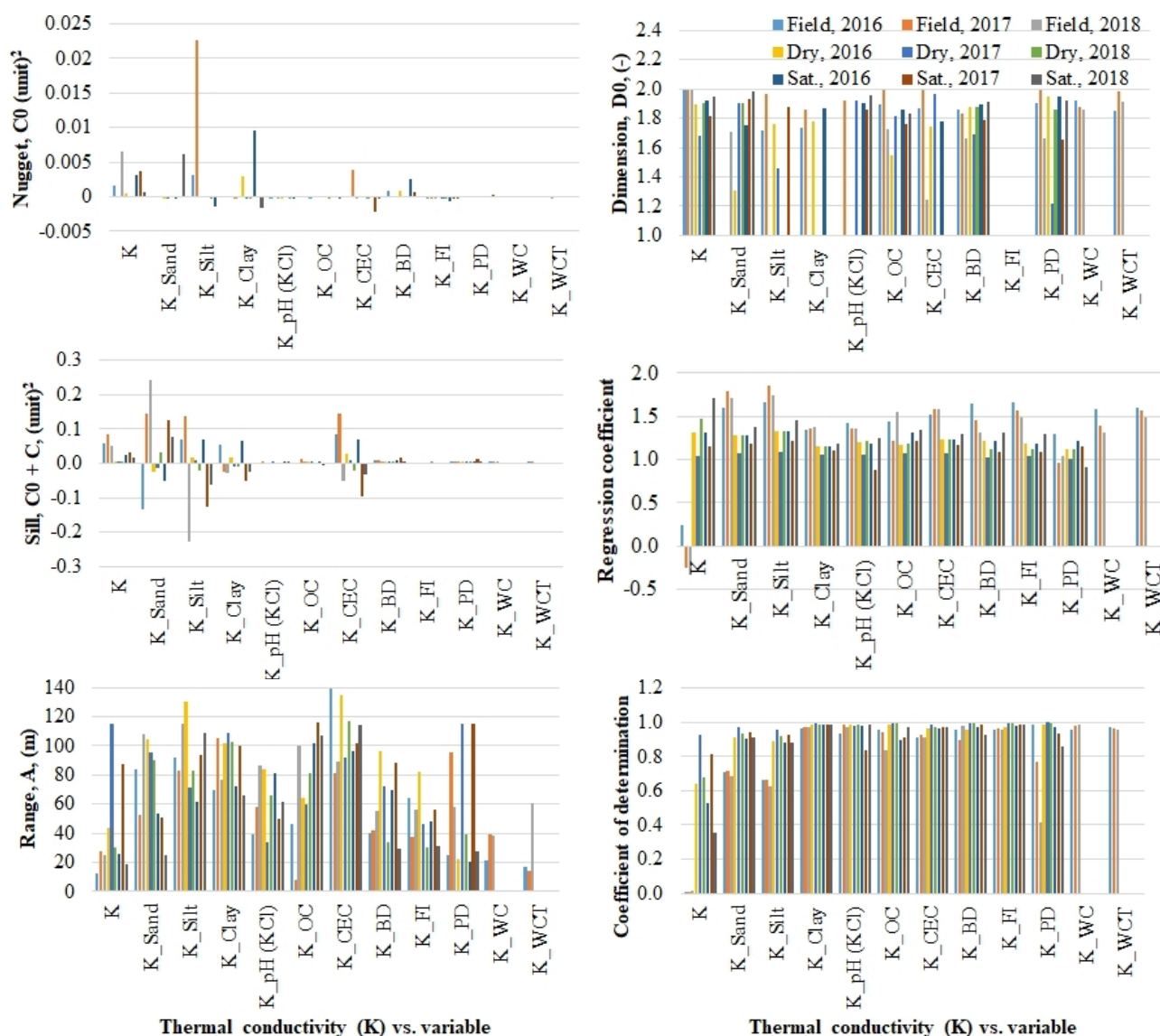


Fig. 3. Parameters of semivariograms of thermal conductivity (K) and cross-semivariograms of thermal conductivity linked with soil variables (sand, silt, and clay contents, pH (KCl), organic carbon (OC), cation-exchange capacity (CEC), bulk density (BD), total porosity (FI), particle density (PD), gravimetric water content (WC), TDR water content (WCT): nugget (C_0), sill ($C_0 + C$), range (A), fractal dimension $D(0)$, regression coefficient, and the coefficient of determination at the current soil water content in the field (Field) and the dry and water-saturated (Sat.) states in 2016, 2017, and 2018.

soil. The mean minimum fractal dimension (1.679) for the thermal properties was respectively greater and lower than those for the stable (1.534) and temporally variable (1.760) soil physical properties. The aforementioned values indicate that the stable soil physical properties contribute less to the variation in thermal properties than the variables modified by SICS application. Among the variable properties, the effect of soil water content was most pronounced (Fig. 7).

The ranges of fractal dimensions for the paired soil thermal and physical properties were 1.528-1.994 (2016), 1.293-1.992 (2017), and 1.211-1.997 (2018) in the field, 1.304-1.973 (2016) 1.219-1.971 (2017), and 1.310-1.903 (2018) in the dry soil, and 1.510-1.975 (2016), 1.301-1.996 (2017), and 1.033-1.984 (2018) in the water-saturated soil

(Figs 3-6). The aforementioned data indicates that the minimum fractal dimensions in the field and in the water-saturated soil decreased in the subsequent study years and remained at a similar level in the dry soil. The maximum fractal dimensions in the field and in the dry and water-saturated soil were similar for all of the study years. The reduction of the fractal dimension in the field in 2017-2018 vs. 2016 as well as the values of the thermal properties is related to lower rainfall in the previous period. A much lower inter-annual differentiation of the fractal dimensions of thermal properties occurred in the dry soil and was attributed to the spatial variability in the stable soil physical properties.

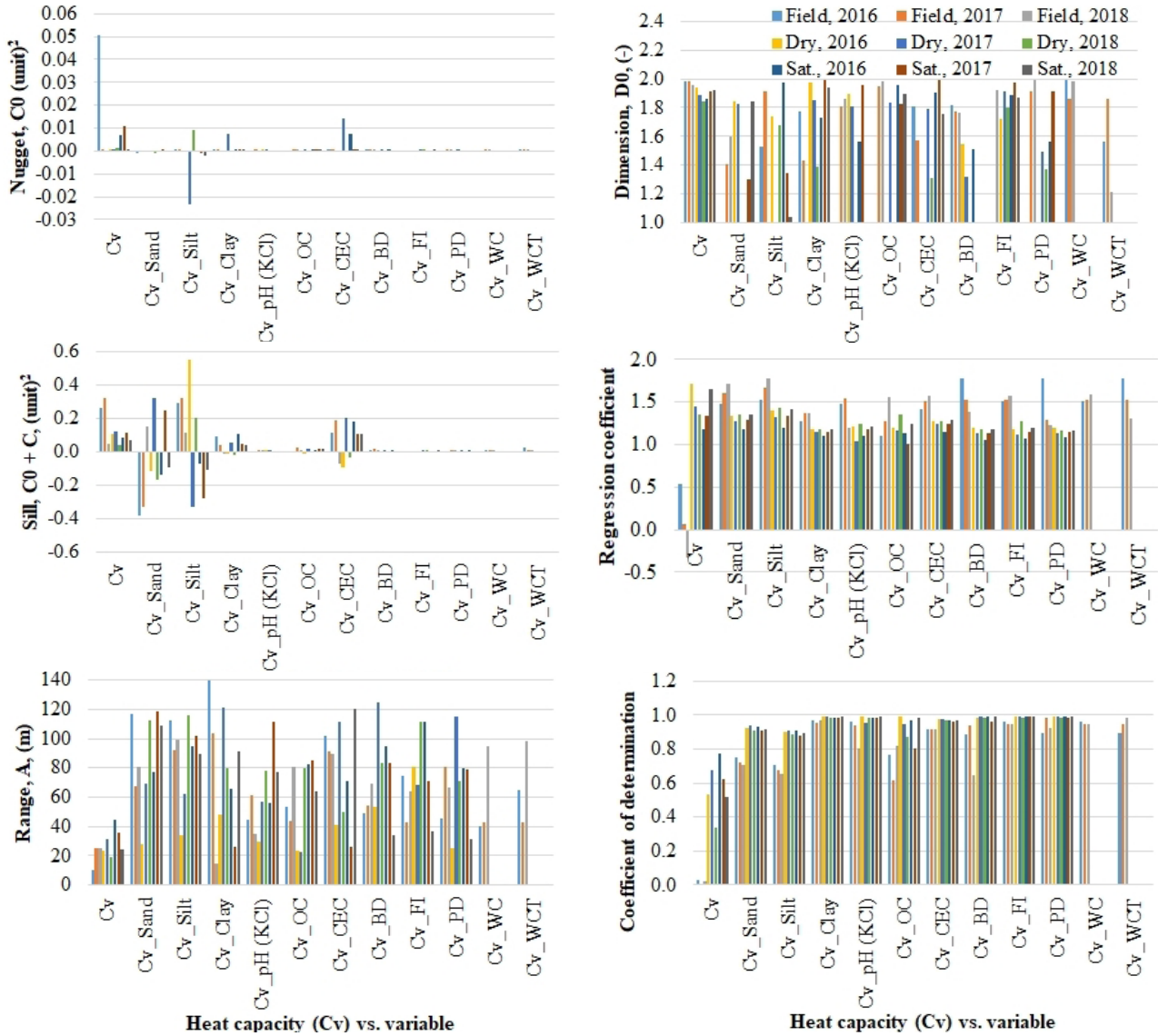


Fig. 4. Parameters of the semivariograms of heat capacity (Cv) and cross-semivariograms of heat capacity linked with soil variables (sand, silt, and clay contents, pH (KCl), organic carbon (OC), cation-exchange capacity (CEC), bulk density (BD), total porosity (FI), particle density (PD), gravimetric water content (WC), TDR water content (WCT): nugget (C_0), sill ($C_0 + C$), range (A), fractal dimension $D(0)$, regression coefficient, and coefficient of determination at the current soil water content in the field (Field) and dry and water-saturated (Sat.) states in 2016, 2017, and 2018.

The results of the OK and OCK methods were validated using the measurement data. The accuracy of the validation was determined by using the linear regression equation coefficients (a) and the coefficient of determination (R^2) (Figs 3-6). The ranges of the regression coefficients (a) and R^2 between the soil properties including sand, silt, clay, OC, pH, and CEC were 0.976-1.547 and 0.09-0.574 for OK and 1.070-1.697 and 0.799-0.988 for OCK, respectively (Usowicz and Lipiec, 2022).

In the case of the variable soil physical properties, including BD, FI, PD, WC, and WCT, the ranges of regression coefficients (a) and R^2 in the OK method were 1.084-1.561 and 0.438-0.966, respectively. The regression coefficients (a) and R^2 for the thermal properties using the OK approach

ranged from -0.413 to 1.752 and 0.001-0.928, respectively. The corresponding ranges for OCK were 0.365-1.869 and 0.164-0.998. The abovementioned parameters indicate that OCK gives more accurate predictions.

Ordinary kriging maps of soil water content obtained using gravimetric and TDR methods were generally similar (Fig. 7) with some exceptions. In the subareas (50-270 m in 2016 and 0-200 m in 2017) with a higher soil bulk density, the values of soil water content were measured using the gravimetric method and their spatial differentiation were higher than those obtained using the TDR method. The mean gravimetric soil water contents in the wet years of 2016 and 2017 ($0.214-0.230 \text{ m}^3 \text{ m}^{-3}$) were higher than those obtained using the TDR method ($0.190-0.205 \text{ m}^3 \text{ m}^{-3}$). In

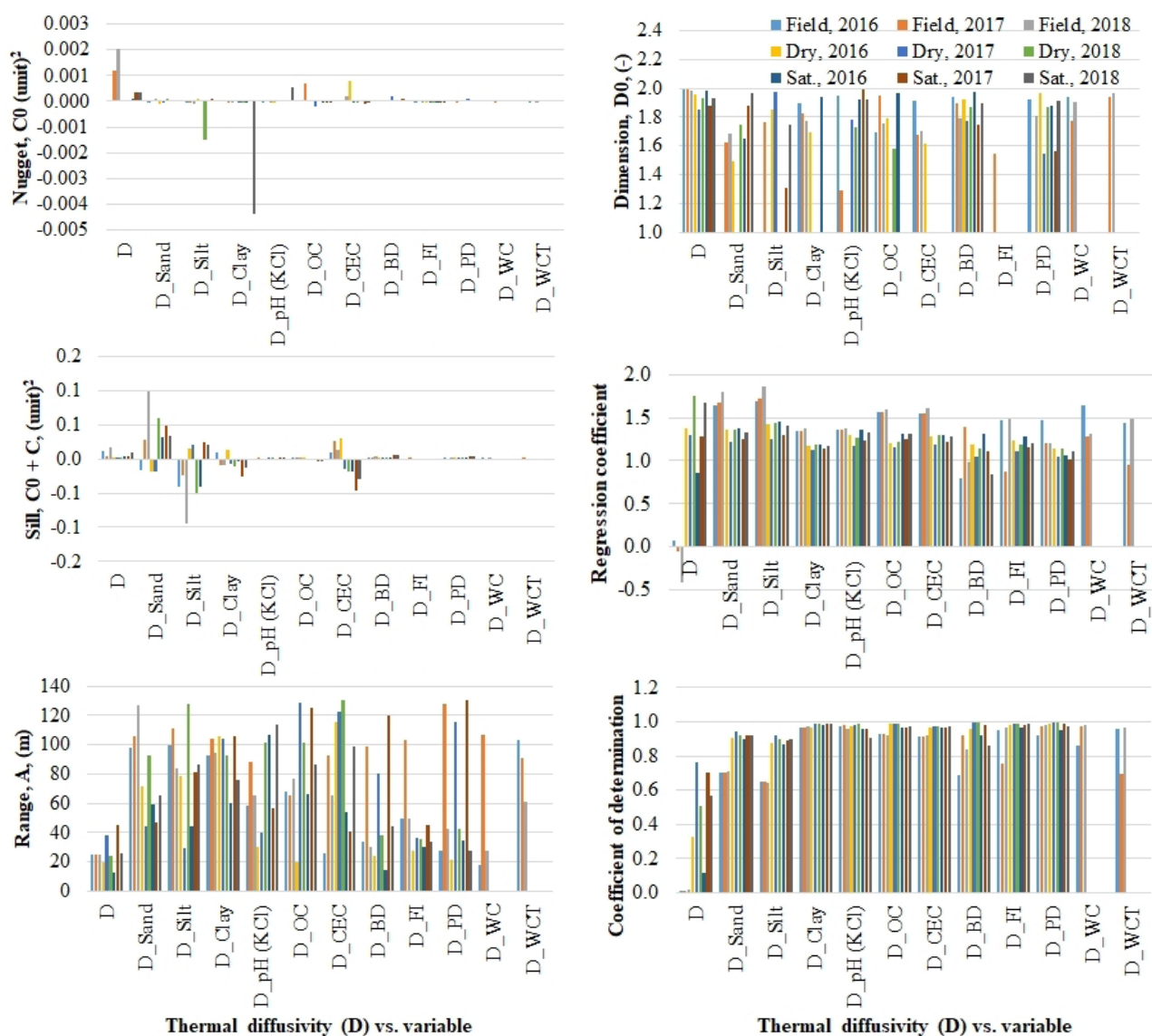


Fig. 5. Parameters of the semivariograms of thermal diffusivity (D) and cross-semivariograms of thermal diffusivity linked with soil variables (sand, silt, and clay contents, pH (KCl), organic carbon (OC), cation-exchange capacity (CEC), bulk density (BD), total porosity (FI), particle density (PD), gravimetric water content (WC), TDR water content (WCT): nugget (C_0), sill ($C_0 + C$), range (A), fractal dimension $D(0)$, regression coefficient, and coefficient of determination at the current soil water content in the field (Field) and dry and water-saturated (Sat.) states in 2016, 2017, and 2018.

the dry year of 2018, the mean gravimetric and TDR soil water contents were $0.091 \text{ m}^3 \text{ m}^{-3}$ and $0.058 \text{ m}^3 \text{ m}^{-3}$ (Table 1, Fig. 7). Overall, the gravimetric method seems to be more sensitive to changes in soil water content in response to SICS application than the TDR method. Irrespective of the measurement method used in 2016 and 2017, the soil water content in the subareas was 40-60, 170-190, and 320-340 m, corresponding to the application of SICS 5 providing the most organic matter. The changes in the water content in response to the other SICS were less pronounced (Fig. 7).

Figure 8 presents the spatial distributions of thermal conductivity, heat capacity, and thermal diffusivity obtained with the OCK method using field-measured data with sand content as the auxiliary variable. Sand (quartz)

was chosen because it improves the predictive potential of OCK through its great influence on the conductivity. The field distributions are related to soil water content and other soil properties. The spatial pattern of the changes differed depending on the soil thermal properties.

As may be observed in Fig. 8, the initial spatial distribution of thermal conductivity (K) at the field soil water content (Fig. 7) in 2016, before the SICS application, was similar to that of the bulk density (BD) (Fig. 9) This is clearly visible in the subarea 120-300 m with increased values of both BD and K. However, there was no such similarity observed in 2017 when the spatial distribution of BD altered upon the SICS application. However, a higher thermal conductivity was recorded in the subarea 100-190 m with the

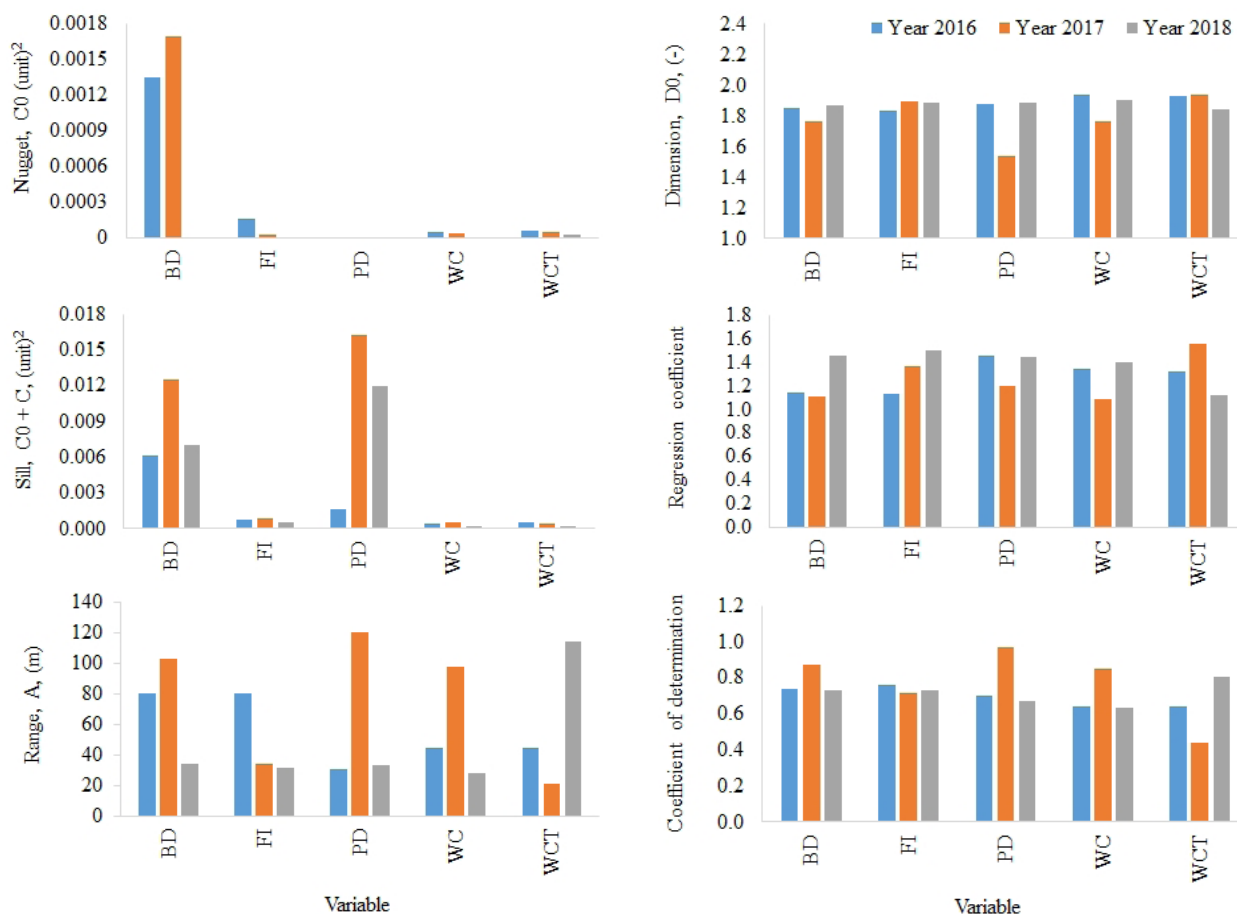


Fig. 6. Semivariogram parameters: nugget (C_0), sill ($C_0 + C$), range (A), fractal dimension $D(0)$, regression coefficient and coefficient of determination for bulk density (BD), total porosity (FI), particle density (PD), gravimetric water content (WC), and TDR water content (WCT) in the experimental field in 2016, 2017, and 2018.

predominance of SICS 3, 4, and 5 including the application of legume catch crops, manure, and their combinations, all providing relatively large quantities of organic matter. This effect was clearly visible in the second and moist (wet) study year (2017) (Fig. 8). In 2018, when the bulk density was reduced by the preceding stubble tilling, the greater K value in the subarea 210-350 m once again corresponded with a higher content of sand (Fig. 10). It is worth noting that the similarity between K and the sand distributions occurred both in the wet (2016) and dry years (2018).

The heat capacity (C_v) distribution did not exhibit a high spatial variation in 2016, whereas in 2017 it increased in subarea 40-190 m corresponding to SICS 3, 4, and 5, which provided the greatest amounts of exogenous organic matter (Fig. 10). However, there was no C_v response to SICS 2 with the lime application. In 2018, the C_v values decreased over the whole experimental field, and the SICS effect was not clearly visible.

The thermal diffusivity (D) distribution in 2016 (Fig. 8) was in part similar to the textural composition (Fig. 6). For example, increased D occurred in the subarea 150-270 m which had a higher sand and silt content. Relatively high values and a small variation of D in response to different bulk densities

indicate that the D values are close to the inflection point (close to the maximum) with the characteristic non-linear response of diffusivity to increasing water content (a rapid increase up to the inflection point and a slower decline afterward) at a given soil bulk density (Mady and Shein, 2016; Usowicz *et al.*, 2016). In 2017, an increased D value was observed in the subareas 0-60 m and 110-140 m with the predominance of SICS 3, 5 and 3, 4, respectively although the D values in the other subareas (150-190 m) with the application of SICS 4 and 5 were rather low and were probably in a zone with a characteristic D decline with increasing soil water content.

Figures 11 and 12 present the spatial distribution of the thermal properties in the dry and water-saturated states that were obtained with the use of the OCK method using laboratory-measured data with sand content as the auxiliary variable. The spatial pattern of the changes differed depending on the type of thermal property, SICS location, and study year.

The spatial distribution of thermal conductivity (K) in the dry and water-saturated states (Figs 11 and 12) was mainly influenced by the distribution of soil bulk density (BD) (Fig. 8). In 2017, the higher values of BD in the subareas 0-190 m and 250-350 m and the lower ones in the subarea 190-250 m were associated with the inherent

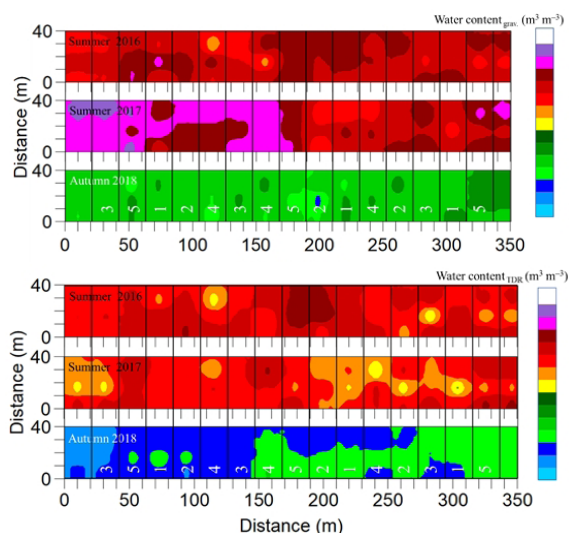


Fig. 7. Spatial distribution of gravimetric water content and water content TDR ($\text{m}^3 \text{m}^{-3}$) in the 0-10 cm layer in the experimental field in 2016, 2017, and 2018. 1 – control, 2 – lime (L), 3 – leguminous catch crops (LU), 4 – farmyard manure (M), and 5 – lime + leguminous catch crops + farmyard manure (L+LU+M).

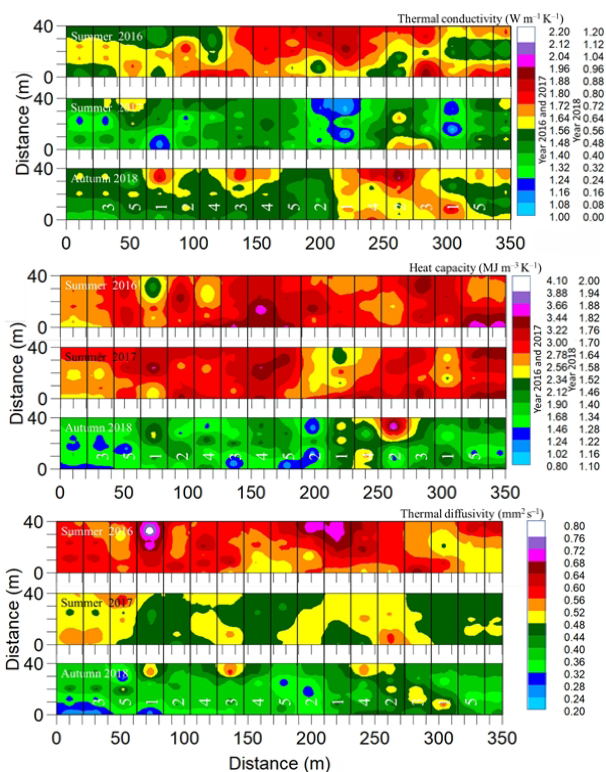


Fig. 8. Spatial distribution of thermal conductivity, heat capacity, and thermal diffusivity in the 0-10 cm layer at the current soil water content in the field in 2016, 2017, and 2018. 1 – control, 2 – lime (L), 3 – leguminous catch crops (LU), 4 – farmyard manure (M), and 5 – lime + leguminous catch crops + farmyard manure (L+LU+M).

textural composition applications of different SICS that were reflected in higher and lower K values, respectively. Additionally, K increased in subareas (20 to 200 m) with a greater silt content (Fig. 10), which may be ascribed to a greater number of contacts between the soil particles. As

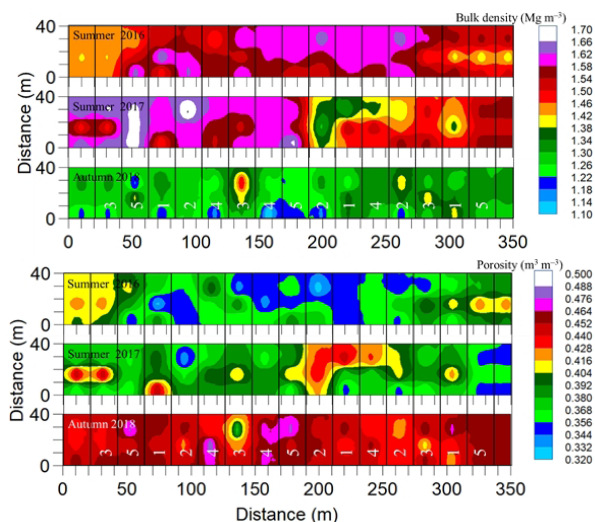


Fig. 9. Spatial distribution of bulk density (Mg m^{-3}) and porosity ($\text{m}^3 \text{m}^{-3}$) in the 0-10 cm layer at the current soil water content in the field in 2016, 2017, and 2018. 1 – control, 2 – lime (L), 3 – leguminous catch crops (LU), 4 – farmyard manure (M), and 5 – lime + leguminous catch crops + farmyard manure (L+LU+M).

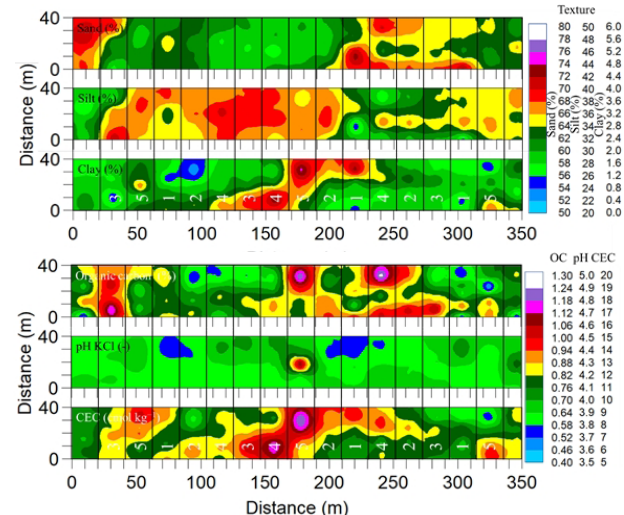


Fig. 10. Spatial distribution of sand (2-0.05 mm), silt (0.05-0.002 mm), clay (<0.002 mm), and organic carbon (OC) in % terms, cation-exchange capacity (CEC) – in cmol kg^{-1} . 1 – control, 2 – lime (L), 3 – leguminous catch crops (LU), 4 – farmyard manure (M), and 5 – lime + leguminous catch crops + farmyard manure (L+LU+M) (Usowicz and Lipiec, 2022).

shown by the measurements, after stubble tilling in 2018, the distribution of BD (and FI values) (Fig. 9) over the whole field with SICS was rather smooth and corresponded with an even K distribution at both soil water states.

The spatial heat capacity (C_v) distributions were more varied in the water-saturated than in the dry state (Figs 11 and 12). Irrespective of the SICS application, the C_v values in the water-saturated state were higher in 2016 and 2017 vs. 2018 when the bulk density values (Figs 7 and 9) were much lower than in the former period. The spatial distribution of soil thermal diffusivity (D) was more diverse in the dry than in the water-saturated soil in all of the studied

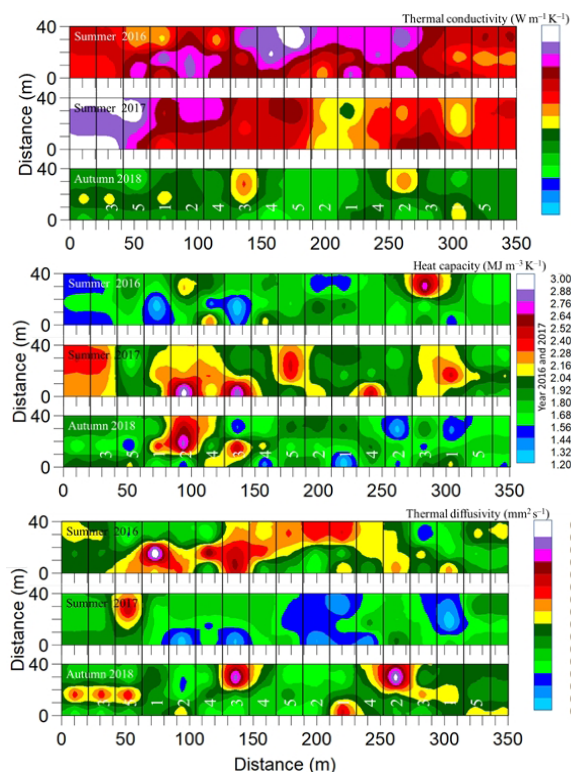


Fig. 11. Spatial distribution of thermal conductivity, heat capacity, and thermal diffusivity in the 0-10 cm layer in the dry state in 2016, 2017, and 2018. 1 – control, 2 – lime (L), 3 – leguminous catch crops (LU), 4 – farmyard manure (M), and 5 – lime + leguminous catch crops (L+LU+M).

years (Figs 11 and 12). The D distribution in both water states resembles that of the bulk density (Figs 7 and 9) to a greater extent in the dry than in the saturated state.

DISCUSSION

The concept of soil-improving cropping systems comprises sustainable management practices to improve soil quality and minimize soil threats (Oenema *et al.*, 2017; Hessel *et al.*, 2022). It includes the application of organic amendments, catch crops, and liming and may be particularly useful for the sustainable improvement of both quality and productivity (Lipiec and Usowicz, 2021; Usowicz and Lipiec, 2022). Various analyses of the kriging-interpolated and cokriging-interpolated maps allowed for the identification of the spatial interrelations between some soil physical properties, thermal properties, and random application of SICS in the farm field in different weather and management (tillage) conditions.

The presence of subareas with similar thermal properties matches with the locations of the selected SICS. One of the subareas (100-190 m) with a higher thermal conductivity consists mainly of SICS 3, 4, and 5, including the application of legume catch crops, manure, and their combinations providing relatively large quantities of organic matter. This effect is clearly visible in the second wet study year (2017) (Fig. 8). Increased thermal conductivity in response to the

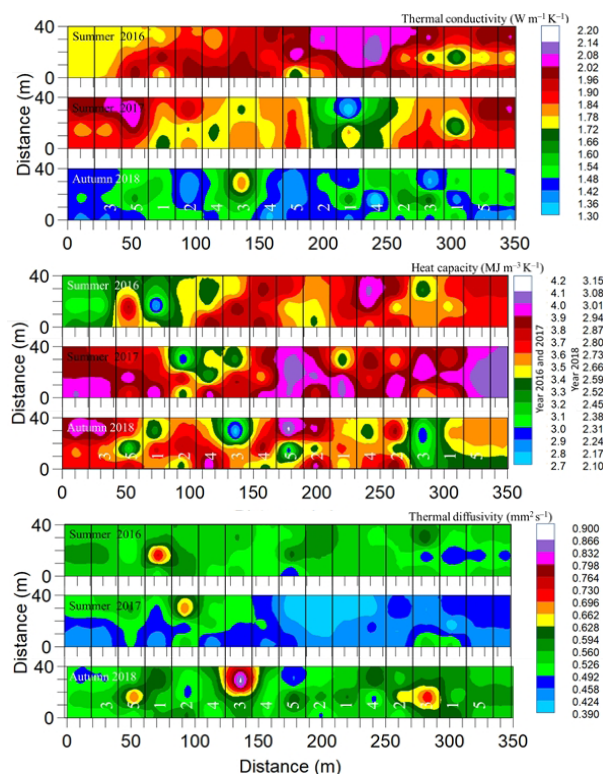


Fig. 12. Spatial distribution of thermal conductivity, heat capacity, and thermal diffusivity in the 0-10 cm layer in the water-saturated soil in 2016, 2017, and 2018. 1 – control, 2 – lime (L), 3 – leguminous catch crops (LU), 4 – farmyard manure (M), and 5 – lime + leguminous catch crops + farmyard manure (L+LU+M).

organic matter supply may be associated with an increase in water-holding capacity and related to the soil water content. The elevated water content in this subarea could additionally be enhanced by the (somewhat) higher content of intrinsic silt and clay at the expense of sand. A similar effect of the three SICS with farmyard manure (M) alone and catch crops (LU) and the combined catch crops with lime and manure (L+LU+M) implies that organic matter from shortfall farmyard manure could be substituted by legume catch crops in order to maintain a comparable response in terms of the thermal conductivity and heat transfer. These results fit with the Greening programme in the EU (Smith *et al.*, 2020) and are aimed at increasing soil carbon stocks in order to combat climate change and improve the supply capacity of nutrients, including legume-fixed atmospheric nitrogen, and warrant sustainable nutrition security (Schjøning *et al.*, 2009; Wysokiński and Kuziemska, 2019). An analysis of the maps of thermal properties and textural composition along with the SICS distribution will help with the selection of the most appropriate management practices with which to modify the thermal conductivity and improve heat transfer and soil temperature required for various soil processes and plant growth.

A comparison of the results between the study years indicated the combined effect of the dry weather conditions and stubble tilling in 2018 which is reflected in a substantial

reduction in the soil thermal properties, in particular heat capacity and thermal diffusivity as compared to those values in 2017. This reduction may be ascribed for the most part to the reduced soil water content and bulk density (Table 1) in 2018 over the whole field area. The decreasing values of the thermal properties with decreasing bulk density and soil water content may be related to the lower number of contacts between thermally conductive soil particles, the lower continuity of conductive water-filled pores (convection and diffusion), and increasing air-filled porosity with extremely low thermal conductivity (Zhang *et al.*, 2021). At the same time, the differences in thermal properties between the SICS in 2018 were masked by the low soil bulk density over the whole field. The effect of the considerably reduced bulk density (or increased total porosity) achieved through stubble tilling alone in 2018 may well be proven with using laboratory measurements, where lower thermal conductivities were obtained at the established dry and water-saturated states (Figs 11 and 12). Another effect of the increased total porosity following tillage in 2018 is the increasing ratios of the mean K and Cv in the water-saturated and dry soil as compared to those in 2016 and 2017 (Table 3). This may be explained by the higher volumetric soil water content at the point of saturation, which corresponds to the greater total porosity.

Table 3. Ratios of K, Cv, and D in water-saturated and dry soil

Year	K _{sat} /dry	Cv _{sat} /dry	D _{sat} /dry
2016*	5.83	2.06	2.77
2017*	5.80	1.47	3.03
2018**	6.99	2.23	3.07

* After harvest before stubble tilling, ** after harvest and stubble tilling.

The analysis of the effective range (spatial dependence), was defined as the distance at which the semivariance value achieves 95% of the sill, and indicated that it was lower for the thermal properties of the *in situ* than for the laboratory measurements. The lower spatial dependence of the thermal properties *in situ* could be influenced for the most part by the effect of the spatially differentiated soil water content and bulk density and the associated air-filled porosity and also by the more stable organic matter content (Abu-Hamdeh and Reeder, 2000; Schjønning, 2021) as well as the textural and mineralogical composition (Usovicz *et al.*, 2020; Roshankhah *et al.*, 2021; Schjønning, 2021). This explanation may be supported by the greater effective ranges in the cross-semivariograms including soil thermal properties as primary variables and sand content as a secondary variable.

Spatial interpolation methods are increasingly being used to generate maps of the thermal soil properties due to the limited availability of measured data. The performance of the interpolation depends on the method applied. Our study showed that the spatial prediction of

soil thermal conductivity, heat capacity, and thermal diffusivity in the cultivated field was more precise using the ordinary cokriging (OCK) method including thermal properties as the main variable and sand as an auxiliary variable ($R^2=0.164-0.998$), as compared to the ordinary kriging (OK) ($R^2=0.001-0.928$). The suitability of the sand content for improving the predictive accuracy of thermal properties (distribution) may be supported by its availability in soil databases (Hengl *et al.*, 2017; Batjes *et al.*, 2020) and the Soil Quality Mobile App (SQAPP) (Fleskens *et al.*, 2020).

CONCLUSIONS

The results of this study showed the following:

1. The spatial variability of thermal properties within the farm field with the random soil-improving cropping systems application of soil-improving cropping systems over the course of a three-year study depended on the type of the thermal property, study year, as well as the weather and management (tillage) conditions. In the second study year (2017) which was wet, from measurements conducted after harvest and before stubble tilling, the values of all thermal properties increased in the subareas with a predominance of SICS providing the largest amounts of organic matter from farmyard manure and/or catch crops but not for soil-improving cropping systems including liming. However, in the dry year of 2018, from measurements carried out after harvest and stubble tilling, the soil-improving cropping systems effect on all the thermal properties was not clearly visible.

2. The spatial distribution of the thermal properties in the experimental field was better described by the cross-semivariograms with auxiliary sand content and ordinary cokriging interpolation as compared to the direct semivariograms and ordinary kriging interpolation.

3. The fractal dimension values indicated that the number of subareas differing in thermal properties in the experimental field was more dependent on the variation in soil density and water content modified by soil-improving cropping systems than on such stable properties of soil as the sand content.

4. The soil-improving cropping systems effect on the spatial distribution of thermal properties was largely masked when measured at extreme water contents, including the water-saturated and dry states. The effect was more pronounced in areas with a higher bulk density which was influenced by both the inherent textural composition, soil-improving cropping systems application, and tillage. The heat capacity was more spatially variable in the water-saturated as opposed to the dry states, whereas the opposite was true for thermal diffusivity. The highest ratios of mean thermal conductivity and heat capacity in the water-saturated and dry soil were recorded in 2018 from measurements conducted after stubble tilling.

5. The cokriging-interpolated maps will help farmers to select the most appropriate management practices with which to modify the thermal properties with the aim of improving heat transfer and the soil temperature required for various soil processes and plant growth.

CRedit authorship contribution statement: B.U. and J.L. performed the experiments and measurements. B.U. carried out the data computation and statistical analysis. Both authors jointly wrote the paper.

Conflict of interest: The authors declare no conflict of interest.

REFERENCES

- Abu-Hamdeh N.H. and Reeder R.C., 2000.** Soil thermal conductivity effects of density, moisture, salt concentration, and organic matter. *Soil Sci. Soc. Am. J.*, 64, 1285-1290, <https://doi.org/10.2136/sssaj2000.6441285x>
- Akter M., Miah M.A., Hassan M.M., Mobin M.N., and Baten M.A., 2015.** Textural influence on surface and subsurface soil temperatures under various conditions. *J. Environ. Sci. Nat. Resour.*, 8(2), 147-151, <https://doi.org/10.3329/jesnr.v8i2.26882>
- Andry H., Yamamoto T., Irie T., Moritani S., Inoue M., and Fujiyama H., 2009.** Water retention, hydraulic conductivity of hydrophilic polymers in sandy soil as affected by temperature and water quality. *J. Hydrol.*, 373, 177-183, <https://doi.org/10.1016/j.jhydrol.2009.04.020>
- Ajayi A.E., Holthusen D., and Horn R., 2016.** Changes in microstructural behaviour and hydraulic functions of biochar amended soils. *Soil Tillage Res.*, 155, 166-175, [doi:10.1016/j.still.2015.08.007](https://doi.org/10.1016/j.still.2015.08.007)
- Batjes N.H., Ribeiro E., and van Oostrum A., 2020.** Standardised soil profile data to support global mapping and modelling (WoSIS snapshot 2019). *Earth Syst. Sci. Data*, 12, 299-320, <https://doi.org/10.5194/essd-12-299-2020>.
- Bialousz S., Marcinek J., Stuczyński T., and Turski R., 2005.** Soil survey, soil monitoring and soil databases in Poland. European Soil Bureau – Research Report No. 9 ESB-RR9, 263-273.
- Blake G.R. and Hartge K.H., 1986.** Bulk density. In: Klute A. (Ed.), *Methods of Soil Analysis*, 546 Part 1: Physical and Mineralogical Methods-Agronomy Monograph No. 9. ASASSA 547, 363-375 (Madison, Wisconsin, U.S.A.), <https://doi.org/10.2136/sssabookser5.1.2ed.c13>
- Bolinder M.A., Crotty F., Elsen A., Frac M., Kismanyoky T., Lipiec J., Tits M., Toth Z., and Kätterer T., 2020.** The effect of crop residues, cover crops, manures and nitrogen fertilization on soil organic carbon changes in agroecosystems: a synthesis of reviews. *Mitig. Adapt. Strateg. Glob. Change*, 25, 929-952, <https://doi.org/10.1007/s11027-020-09916-3>
- Bronick C.J. and Lal R., 2005.** Manuring and rotation effects on soil organic carbon concentration for different aggregate size fractions on two soils in northeastern Ohio, USA. *Soil Tillage Res.*, 81, 239-252, <https://doi.org/10.1016/j.still.2004.09.011>
- Cambardella C.A., Moorman T.B., Parkin T.B., Karlen D.L., Novak J.M., Turco R.F., and Konopka A.E., 1994.** Field-scale variability of soil properties in Central Iowa soils. *Soil Sci. Soc. Am. J.*, 58, 1501-1511, <https://doi.org/10.2136/sssaj1994.03615995005800050033x>
- Dahiya I.S., Ritcher J., and Mark P.S., 1984.** Soil spatial variability: review. *Int. J. Trop. Agric.*, 11, 1-102.
- Dec D., Dörner J., and Horn R., 2009.** Effect of soil management on their thermal properties. *J. Plant Nutr. Soil Sci.*, 9, 26-39, <https://doi.org/10.4067/S0718-27912009000100003>
- Fleskens L., Ritsema C., Bai Z., Geissen V., Mendes de Jesus J., da Silva V., Teeuwen A., and Yang X., 2020.** Tested and validated final version of SQAPP. 143 ppiSQAPER Project Deliverable 4.2. The Soil Quality Mobile App (SQAPP), www.isqaper-is.eu.
- Gamage D.N.V., Biswas A., and Strachan I.B., 2019.** Spatial variability of soil thermal properties and their relationships with physical properties at field scale. *Soil Tillage Res.*, 193, 50-58, <https://doi.org/10.1016/j.still.2019.05.012>
- Gliński J. and Lipiec J., 1990.** *Soil Physical Conditions and Plant Roots*. 260 pp, First Published 1st edition. CRC Press Reissued 2018 by CRC Press Taylor & Francis Group.
- He H., Liu L., Dyck M., Si B., and Lv J., 2021.** Modelling dry soil thermal conductivity. *Soil Tillage Res.*, 213, 105093, <https://doi.org/10.1016/j.still.2021.105093>
- Heitman J.L., Horton R., Ren T., Nassar I.N., and Davis D.D., 2008.** A test of coupled soil heat and water transfer prediction under transient boundary temperatures. *Soil Sci. Soc. Am. J.*, 72 (5), 1197-1207, <https://doi.org/10.2136/sssaj2007.0234>
- Heitman J., Zhang X., Xiao X., Ren T., and Horton R., 2020.** Advances in heat-pulse methods: Measuring soil water evaporation with sensible heat balance. *Soil Sci. Soc. Am. J.*, 84, 1371-1375, <https://doi.org/10.1002/saj2.20149>
- Hengl T., Mendes de Jesus J., Heuvelink G.B.M., Ruiperez-Gonzalez M., Kilibarda M., Blagotić A., Shangguan W., Wright M.N., Geng X., Bauer-Marschallinger B., Guevara M.A., Vargas R., MacMillan R.A., Batjes N.H., Leenaars J.G.B., Ribeiro E., Wheeler I., Mantel S., and Kempen B., 2017.** SoilGrids250m: global gridded soil information based on machine learning. *PLoS ONE*, 12 (2), e0169748, <https://doi.org/10.1371/journal.pone.0169748>
- Hessel R., Wyseure G., Panagea I., Alaoui A., Reed M.S., van Delden H., Muro M., Mills J., Oenema O., Areal F., van den Elsen E., Verzaandvoort S., Assinck F., Elsen A., Lipiec J., Koutroulis A., O'Sullivan L., Bolinder M., Fleskens L., Kandel E., Montanarella L., Heinen M., Toth Z., Hallama M., Cuevas J., Baartman J., Piccoli I., Dalgaard T., Stolte J., Black J., and Chivers C., 2022.** Soil improving cropping systems for sustainable and profitable farming in Europe. *Land*, 11(6), 780, <https://doi.org/10.3390/land11060780>
- ISO, 1995.** International Organization for Standardization 13536: Soil Quality – Determination of the Potential Cation Exchange Capacity and Exchangeable Cations Using Barium Chloride Solution Buffered at pH (7 pp).
- Jankowski M., Przewoźna B., and Bednarek R., 2011.** Topographical inversion of sandy soils due to local conditions in Northern Poland. *Geomorphology (Amst)*, 135, 277-283, <https://doi.org/10.1016/j.geomorph.2011.02.005>
- Keiblinger K.M., Lisa M., Bauer M., Deltedesco E., Holawe F., Unterfrauner H., Zehetner F., and Peticzka R., 2016.** Quicklime application instantly increases soil aggregate stability. *Int. Agrophys.*, 30(1), 123-128, <https://doi.org/10.1515/intag-2015-0068>
- Krasowicz S., Oleszek W., Horabik J., Dębicki R., Jankowiak J., Stuczyński T., and Jadczyński J., 2011.** Rational management of the soil environment in Poland. *Pol. J. Agron.*, 7, 43-58.

- Lal R., 2020.** Soil organic matter and water retention. *Agron. J.*, 112, 3265-3277, <https://doi.org/10.1002/agj2.20282>
- Lipiec J. and Hatano R., 2003.** Quantification of compaction effects on soil physical properties and crop growth. *Geoderma*, 16, 107-136, [https://doi.org/10.1016/S0016-7061\(03\)00097-1](https://doi.org/10.1016/S0016-7061(03)00097-1)
- Lipiec J., Nosalewicz A., and Pietrusiewicz J., 2011.** Crop responses to soil physical conditions. In: *Encyclopedia of Agrophysics* (Eds J. Gliński, J. Horabik, and J. Lipiec), 167-176, Springer Dordrecht, Heidelberg, London, New York, https://doi.org/10.1007/978-90-481-3585-1_36
- Lipiec J. and Uowicz B., 2021.** Quantifying cereal productivity on sandy soil in response to some soil-improving cropping systems. *Land*, 10(11), 1199, <https://doi.org/10.3390/land10111199>
- Liu Z., Xu J., Li X., and Wang J., 2018.** Mechanisms of biochar effects on thermal properties of red soil in south China. *Geoderma*, 323, 41-51, <https://doi.org/10.1016/j.geoderma.2018.02.045>
- Mady A.Y. and Shein E.V., 2016.** Modeling soil thermal diffusivity as a function of soil moisture. *Bull. Orenburg State Univ.*, 12(200), 56-60.
- Mellander P.E., Bishop K., and Lundmark T., 2004.** The influence of soil temperature on transpiration: a plot scale manipulation in a young scots pine stand. *For. Ecol. Manag.*, 195, 15-28, <https://doi.org/10.1016/j.foreco.2004.02.051>
- Mitchell-Forsyth B., Haruna S., and Downs K., 2021.** Variability of soil thermal properties along a catena in Middle Tennessee, USA. *Int. Agrophys.*, 35(2), 209-219. <https://doi.org/10.31545/intagr/140079>
- Nagihara S., Hedlund M., Zacny K., and Taylor P.T., 2014.** Improved data reduction algorithm for the needle probe method applied to in-situ thermal conductivity measurements of lunar and planetary regoliths. *Planet. Space Sci.*, 92, 49-56, <https://doi.org/10.1016/j.pss.2013.12.012>
- Novák P., Chyba J., Kumhála F., and Procházka P., 2014.** The measurement of stubble cultivator draught force under different soil conditions. *Agron. Res.*, 12, 135-142.
- Ochsner T.E., Horton R., and Ren T., 2001.** A new perspective on soil thermal properties. *Soil Sci. Soc. Am. J.*, 65, 1641-1647, <https://doi.org/10.2136/sssaj2001.1641>
- Ochsner T.E., Sauer T.J., and Horton R., 2007.** Soil heat capacity and heat storage measurements in energy balance studies. *Agron. J.*, 99, 311-314, <https://doi.org/10.2134/agronj2005.0103S>
- Oenema O., Heinen M., Rietra R., and Hessel R., 2017.** A review of soil-improving cropping systems: Wageningen Environmental Research, Scientific Report 06, 1-59.
- Ostrowska A., Gawliński S., and Szczubiałka Z., 1991.** Analyses and Evaluation Methods of Soil and Plants (in Polish). Institute of Environmental Protection, Warsaw, p. 334.
- Peng S., Piao S., Wang T., Sun J., and Shen Z., 2009.** Temperature sensitivity of soil respiration in different ecosystems in China. *Soil Biol. Biochem.*, 41, 1008-1014. doi:10.1016/j.soilbio.2008.10.023
- Reichert J.M., Albuquerque J.A., Kaiser D.R., Reinert D.J., Urach F.L., and Carlesso R., 2009.** Estimation of water retention and availability in soils of Rio Grande do Sul. *Rev. Bras. Cienc. Solo*, 33, 1547-1560, <https://doi.org/10.1590/S0100-06832009000600004>
- Robertson G.P., 2008.** GS+: Geostatistics for the Environmental Sciences. Gamma Design Software, Plainwell, MI, USA.
- Roshankhah S., Garcia A.V., and Santamarina J.C., 2021.** Thermal conductivity of sand-silt mixtures. *J. Geotech. Geoenviron. Eng.*, 147(2), 06020031, [https://doi.org/10.1061/\(ASCE\)GT.1943-5606.0002425](https://doi.org/10.1061/(ASCE)GT.1943-5606.0002425)
- Rutkowska A. and Pikula D., 2013.** Effect of crop rotation and nitrogen fertilization on the quality and quantity of soil organic matter. In: *Soil Processes and Current Trends in Quality Assessment* (Ed. M.C. Hernandez Soriano). Intech Open, 249-267, <https://doi.org/10.5772/53229>
- Schjønning P., 2021.** Thermal conductivity of undisturbed soil – Measurements and predictions. *Geoderma*, 402, 115188. <https://doi.org/10.1016/j.geoderma.2021.115188>.
- Schjønning P., Heckrath G., and Christensen B.T., 2009.** Threat to soil quality in Denmark. A review of existing knowledge in the context of the EU soil thematic strategy. In DJF Report Plant Science no. 143; Aarhus University: Tjele, Denmark, 11-121. <http://web.agrsci.dk/djfpublikation/index.asp?action=show&id=1073>
- Smith P., Soussana J.-F., Angers D., Schipper L., Chenu C., Rasse D.P., Batjes N.H., van Egmond F., McNeill S., Kuhnert M., and Arias-Navarro C., 2020.** How to measure, report and verify soil carbon change to realize the potential of soil carbon sequestration for atmospheric greenhouse gas removal. *Glob. Change Biol. Bioenergy*, 26, 219-241, <https://doi.org/10.1111/gcb.14815>
- Soussana J.-F., Lutfalla S., Ehrhardt F., Rosenstock T., Lamanna C., Havlík P., Richards M., Wollenberg E., Chotte J.-L., Torquebiau E., Ciaï P., Smith P., and Lal R., 2017.** Matching policy and science: Rationale for the ‘4 per 1000 – soils for food security and climate’ initiative. *Soil Tillage Res.*, 188, 3-15, <https://doi.org/10.1016/j.still.2017.12.002>
- Tarnawski V.R., Wagner B., Leong W.H., McCombie M., Coppa P., and Bovesecchi G., 2021.** Soil thermal conductivity model by de Vries: Re-examination and validation analysis. *Eur. J. Soil Sci.*, 72(5), 1940-1953, <https://doi.org/10.1111/ejss.13117>
- Thorsen M.K., Hopkins D.W., Woodward S., and McKenzie B.M., 2010.** Resilience of microorganisms and aggregation of a sandy calcareous soil to amendment with organic and synthetic fertilizer. *Soil Use Manage.*, 26, 149-157, <https://doi.org/10.1111/j.1475-2743.2010.00262.x>
- Uowicz B., 1995.** Evaluation of methods for soil thermal conductivity calculations. *Int. Agrophysics.*, 9(2), 109-113.
- Uowicz B., Hajnos M., Sokolowska Z., Józefaciuk G., Bowanko G., and Kosowski J., 2004.** Spatial variability of physical and chemical soil properties in a field and commune scale (in Polish). *Acta Agroph.*, 103, 237-247.
- Uowicz B., Lipiec J., and Uowicz J.B., 2008.** Thermal conductivity in relation to porosity and hardness of terrestrial porous media. *Planet. Space Sci.*, 56, 438-447, <https://doi.org/10.1016/j.pss.2007.11.009>
- Uowicz B., Lipiec J., Uowicz J., and Marczewski W., 2013.** Effects of aggregate size on soil thermal conductivity: comparison of measured and model-predicted data. *Int. J. Heat Mass Transf.*, 57, 536-541, <https://doi.org/10.1016/j.ijheatmasstransfer.2012.10.067>
- Uowicz B., Lipiec J., Łukowski M., Marczewski W., and Uowicz J., 2016.** The effect of biochar application on thermal properties and albedo of loess soil under grassland and fallow. *Soil Tillage Res.*, 164, 45-51, <https://doi.org/10.1016/j.still.2016.03.009>
- Uowicz B. and Lipiec J., 2017.** Spatial variability of soil properties and cereal yield in a cultivated field on sandy soil. *Soil Tillage Res.*, 174, 241-250, <https://doi.org/10.1016/j.still.2017.07.015>

- Usovicz B., Lukowski M.I., Rudiger C., Walker J.P., and Marczewski W., 2017.** Thermal properties of soil in the Murrumbidgee River Catchment (Australia). *Int. J. Heat Mass Transf.*, 115, 604-614, <https://doi.org/10.1016/j.ijheatmasstransfer.2017.08.021>
- Usovicz B. and Lipiec J., 2019.** The effect of exogenous organic matter on the thermal properties of tilled soils in Poland and the Czech Republic. *J. Soils Sediments*, 20, 365-379, <https://doi.org/10.1007/s11368-019-02388-2>
- Usovicz B., Lipiec J., Lukowski M., Bis Z., Usovicz J., and Latawiec A.E., 2020.** Impact of biochar addition on Murrumbidgee River Catchment soil thermal properties: Modelling approach. *Geoderma*, 376, 114574, <https://doi.org/10.1016/j.geoderma.2020.114574>
- Usovicz B. and Lipiec J., 2022.** Assessment of the spatial distribution of cereal yields on sandy soil related to the application of soil-improving cropping systems (SICS). *Sci. Total Environ.*, 830, 154791, <https://doi.org/10.1016/j.scitotenv.2022.154791>
- WRB IUSS Working Group., 2015.** World reference base for soil resources 2014, update 2015. International Soil Classification System for Naming Soils and Creating Legends for Soil Maps. World Soil Resources Reports No. 106, FAO, Rome.
- Wysokiński A. and Kuziemska B., 2019.** The sources of nitrogen for yellow lupine and spring triticale in their intercropping. *Plant Soil Environ.*, 65, 145-151, <https://doi.org/10.17221/644/2018-PSE>
- Valkama E., Lemola R., Känkänen H., and Turtola E., 2015.** Meta-analysis of the effects of under sown catch crops on nitrogen leaching loss and grain yields in the Nordic countries. *Agric. Ecosyst. Environ.*, 203, 93-101, <https://doi.org/10.1016/j.agee.2015.01.023>
- Xu X., Luo Y., and Zhou J., 2012.** Carbon quality and the temperature sensitivity of soil organic carbon decomposition in a tallgrass prairie. *Soil Biol. Biochem.*, 50, 142-148, <https://doi.org/10.1016/j.soilbio.2012.03.007>
- Yost J.L. and Hartemink A.E., 2019.** Chapter four – Soil organic carbon in sandy soils: A review. *Adv. Agron.*, 158, 217-230, <https://doi.org/10.1016/bs.agron.2019.07.004>
- Zaniewicz-Bajkowska A., Rosa R., Kosterna E., and Franczuk J., 2013.** Catch crops for green manure biomass yield and macroelement content depending on the sowing date. *Acta Sci. Pol., Agricultura*, 12 (1), 65-79.
- Zhao Y. and Sia B., 2019.** Thermal properties of sandy and peat soils under unfrozen and frozen conditions. *Soil Tillage Res.*, 89, 64-72, <https://doi.org/10.1016/j.still.2018.12.026>
- Zhang Z., Zhang F., and Muhammed R.D., 2021.** Effect of air volume fraction on the thermal conductivity of compacted bentonite materials. *Engineering Geology*, 284, 106045, <https://doi.org/10.1016/j.enggeo.2021.106045>